Active excitation and damping rate measurement of intermediate-n Toroidal Alfvén Eigenmodes in JET, C-Mod and MAST plasmas

A.Fasoli[1], D.Testa[1], T.Panis[1], A.Klein[2], J.A.Snipes[2], J.Sears[2], M.Gryaznevich[3], R.Martin[3], S.D.Pinches[3], and JET-EFDA contributors[*]

[1]*CRPP, Association EURATOM–Confédération Suisse, EPFL, 1015 Lausanne, Switzerland*
[2]*MIT Plasma Science and Fusion Center, Cambridge, MA 02139, USA*
[3]*Euratom-UKAEA Fusion Association, Culham Science Centre, Abingdon, UK*

Abstract

The stability properties of Alfvén Eigenmodes (AEs) are investigated directly using external antenna excitation and detection of stable modes in a variety of plasma configurations in different devices. Dedicated methods to measure the AE damping rate separately from the fast ion drive have been pioneered at JET, using low toroidal mode number internal saddle coil antennas. Other experiments have since installed localised in-vessel antennas to drive and detect MHD modes in the Alfvén frequency range, first on C-Mod, then on MAST. Experiments on C-Mod proved for the first time that intermediate-n TAEs can be driven and detected, and point out significant differences with respect to the low-n regime on JET in the values and scaling of the damping rate with plasma parameters, e.g. the edge shape. On JET, a new antenna system, comprising two assemblies of four toroidally spaced coils each, was developed to replace the low-n saddle coil structure and excite AE modes in the toroidal mode number range that is expected to be most unstable in ITER, with n up to ~10. Experiments with the new JET antennas confirm that excitation is possible in a large volume plasma, together with real time tracking of core modes throughout the limiter and divertor phases of high performance discharges, with significant additional heating. The similarities and differences between the active MHD antenna systems, as well as a comparison of the results on C-Mod, JET and MAST are illustrated. Both C-Mod and JET results underline the fact that a precise reconstruction of the mode structure and its spectrum, important for a quantitative comparison with theoretical models, represents a significant challenge in the intermediate-n range and in the presence of several modes.

[*] Annex 1 of M.L.Watkins, "*Overview of JET Results*", 21st IAEA Fusion Energy Conference, Chengdu, 2006.

1. Introduction

The stability properties of Alfvén Eigenmodes (AEs) and their potential effect on the distribution of fast ions, including fusion generated α's, are among the most important building blocks for the physics of burning plasmas that can be addressed in present devices [1,2]. A fundamental role for the stability, but also for the nonlinear developments, is played by the damping rate of the mode [3]. The predictions for ITER stability against fast ion driven modes rely on estimates of the AE total damping rate resulting from the contribution of different mechanisms, such as the interaction with [4,5], and the tunnelling to [6], the shear Alfvén continuum, the interaction with the dynamics of the particles' orbit de-trapping [7], and the ion [8] and electron [9] Landau damping. These mechanisms can originate both from the background plasma and the fast ion populations.

Very significant progress has been achieved in understanding the physics of fast ion driven modes in the Alfvén range of frequencies and of their interaction with the background plasma and the fast ion populations themselves. Recent breakthroughs have been achieved for example in the measurement of the spatial structure of unstable AEs [10], the fast ion redistribution in the presence of many AEs [11], and the AE induced fast ion losses [12]. However, a precise validation of the quantitative model of each of the individual damping mechanisms, and their significance in different ITER and DEMO relevant scenarios, is still missing. In particular, although very large amounts of data on AE damping rates exist from JET experiments using low toroidal mode number (n) antennas, these do not cover the range that is anticipated to be the most unstable in ITER [13]. Moreover, only relatively sporadic comparisons with theory have been conducted in the past [14-17].

These considerations lead to two complementary ways of approaching the problem. One way is to improve the framework for comparing theory and experiment, now that the numerical codes contain most physics ingredients to describe the various damping mechanisms. The second is to establish a database of measurements of intermediate-n damping rates in a variety of configurations. These two approaches constitute essential elements for the validation of predictions of ITER and DEMO stability with respect to the fast ion driven modes. This paper focuses on the second approach. In order for such database to provide sufficiently stringent tests for the theory, measurements need to be taken in a variety of configurations and plasma scenarios, ideally in different devices. This has indeed been the case in recent times. After the pioneering experiments on JET using the low-n saddle coils, medium-n antenna structures were installed in a number of different devices for the excitation and detection of modes in the Alfvén frequency range, a technique known as *active MHD spectroscopy* [18]. Alcator C-

Mod first [19], then JET itself, with a new set of localised antennas [20], MAST [21] and, more recently, JT-60U [22] have all installed in-vessel active MHD spectroscopy antennas.
In this paper we briefly review the method of active MHD spectroscopy to investigate the AE stability and we summarise the results on their linear stability of low-n modes. Then, we discuss the active MHD spectroscopy antennas of C-Mod, JET and MAST, illustrating the main recent results. We also discuss the similarities and differences between different devices, focussing in particular on the experimental results obtained on JET and C-Mod. Common issues for interpreting the data and using it for extrapolating to ITER are discussed in the conclusions and outlook Section.

2. Active MHD spectroscopy for linear AE stability studies

The first active antenna system for the study of the AE stability was installed on JET. Several requirements were identified for an active MHD diagnostic that would be able to drive and detect modes in the AE frequency range, corresponding roughly to 20-500kHz for JET, the most important one being the need for in-vessel antennas. To this end, the previously installed saddle coils, which were originally dedicated to disruption feedback stabilization and error field control, were also employed for active MHD spectroscopy. Each coil (now disconnected and essentially dismantled) was made of three turns of a large cross-section Inconel 600 conductor and covered about 90^0 toroidally and 60^0 poloidally, with a self-inductance of about 25μH [23].
The AE excitation system, which has remained practically the same for the new antennas described in Section 5, includes a 5kW broadband power amplifier, an impedance matching network, a power splitter (distribution unit) and an isolation unit. The power control system includes a number of functions used to monitor (and trip the plant in case of) possible electrical faults, such as earth faults and turn-to-turn shorts. The power distribution unit can drive different combinations of antenna phasing (+ and –) for 1, 2 or 4 antennas. Because of their geometrical arrangement, the JET saddle coils preferentially excited low toroidal mode numbers (typically $|n|=0, 1, 2$). The maximum current and voltage applied to the saddle coils were of the order of 20A and 600V, leading to a maximum power coupled to the modes of the order of a kW. The corresponding magnetic perturbations in the plasma core, $|\delta B/B|<10^{-6}$, were too low to significantly affect the transport of energetic particles. As expected, the coupling to the modes of the same toroidal mode number is observed, on JET and on the other devices using active antennas to drive AEs, to depend on the distance between the antenna and the mode resonance surface.

For all active MHD experiments, the plasma response during repetitive sweeps of the antenna driving frequency is determined in terms of driven oscillating quantities such as magnetic fields and densities, extracted from background noise via synchronous detection of signals primarily from magnetic coils, but also including ECE, heterodyne reflectometer (O- and X-mode) and X-ray fast cameras. The diagnostic signals are multiplied by a reference signal, then are low-pass filtered. The reference signal typically corresponds to the injected current and is transmitted optically to the different areas of the plant where the diagnostic signals are acquired. The in-phase and quadrature (I and Q, respectively) signals result from the multiplication with the reference signal itself (I) and with its 90^0 out of phase component (Q) and, once properly normalized (typically to the antenna current), correspond to the real and imaginary parts of the antenna-plasma transfer function $H(\omega,r)$. By fitting the measured transfer function for a number of probes with a rational function $H(\omega,r)=B(\omega,r)/A(\omega)$, one obtains the mode frequency, damping rate γ/ω and (residue) amplitude for the different channels (e.g., providing a radial profile) [24]. Note that the linearity of the system makes the measured damping independent of the magnitude of the drive and of the coupling.

Synchronous detection is performed analogically on JET. The transfer function $H(\omega,r)$ is digitized at 1.5kHz rate for 12sec. The frequency resolution is better than 100Hz, with frequency sweep rates of the order of 200kHz/sec. With recent improvements in the direct digitization of the fluctuating signals, in terms of sampling rate (up to 2MHz at present on JET), dynamic range (14bits), and memory depth (up to 32sec of data acquisition at 2MHz), synchronous detection can also be performed post-pulse on the digital signals. This is the technique employed on the active MHD system in use on Alcator C-Mod [19], which will be discussed in more details in Section 4. JET results confirm that the AE frequencies and damping rates reconstructed with the two methods (analogue and digital) are nearly identical [25], within the typical small error bars, usually smaller than 1% in the mode frequency and of the order of 10% in the damping rate.

The existence of stable Alfvén Eigenmodes of weak damping ($\gamma/\omega<10\%$) was very clearly demonstrated since the very first experiments using the JET active MHD system [24, 26], confirming the MHD theory to a very high degree of accuracy. No other resonant modes were found in the plasma spectrum in the Alfvén wave frequency range (20-500kHz) in the absence of energetic particles. Figure 1 shows an example of a plasma resonance corresponding to an n=1 Toroidal AE (TAE). A clear signature of the TAE resonance is visible on the impedance signal, measured at two different points along the power transmission line. An Eigenmode

corresponds typically to a variation in the loading of up to a few Ohms. Note that this parameter provides indeed a practical way of detecting the Eigenmodes in numerical simulations, to determine coupling and even damping rates. In practice, in the codes a virtual antenna is inserted and its loading as a function of frequency is computed [27].

This data confirms that modes of global nature can be coupled with external antennas, and that extremely high signal-to-noise ratios can in principle be achieved. The neatness of the plasma response is due to the measurement technique, to the robustness of the MHD modes in the plasma, and to the fact that the plasma spectrum is generally exempt from high activity turbulence levels in this range of frequency. A very accurate determination of the mode parameters (frequency, damping rate and, when internal fluctuation measurements are available in the appropriate frequency range, radial structure) [24] is therefore possible, opening the way, more generally, for a very precise *MHD spectroscopy* [18].

The potential of the JET AE active diagnostic is significantly enhanced by the application of a digital real time control system to perform individual resonance tracking, the so-called *Alfvén Eigenmode Local Manager* (AELM). The controller of the exciter frequency, which runs at a 1ms clock rate, varies the frequency linearly around the expected frequency of the mode (f_{AE}), calculated in real time from the measured density and magnetic field. The frequency f_{AE} corresponds to the centre of the gap for the chosen class of Eigenmodes, which is used as a first guess for the eigenfrequency, and should be calculated from the local value of the density, magnetic field and safety factor. In most experimental conditions, for the low-n modes driven by the saddle coils and also for the medium-n modes driven with the new antennas, the line averaged density divided by the major radius was used, together with q=1.5, to provide an initial real-time estimate for the mode frequency in the AELM algorithm. A frequency multiplier that is assumed to be proportional to the total plasma current is used to account for the variation of the safety factor within a discharge.

When an AE resonance is met, the exciter frequency is swept back and forth around the resonance full width. As a result, the AE frequency and damping rate can be measured in real time with high time resolution (typically <30ms) along their dynamical evolution throughout a JET discharge. Real time discrimination of the driven and detected toroidal mode numbers via the AELM resonance detection software is also possible when connecting to the data server the synchronous data for different pick-up coils. For the old saddle coil system, as just two coils at toroidally opposite locations were acquired in real-time, only n-odd vs. n-even modes could be separated. For the new antenna system, eight pick-up coils are connected to the AELM, allowing for a more precise real-time discrimination of toroidal mode numbers.

Finally, a simple algorithm was developed to obtain in real-time the mode frequency and the damping rate from the width of the AELM frequency sweep, using the phase inversion characteristic of a stable, antenna-driven, plasma resonance. The real-time measurements are in very good agreement with the values computed post-discharge [28].

Stable AEs of different nature (Global AEs – GAEs, TAEs, Elliptic AEs – EAEs and Non-Circular AEs – NAEs) have been routinely driven with the saddle coils and detected in JET ohmic plasmas in the range 80-500kHz, with measured damping rates covering a large range, $0.1\% < \gamma/\omega < 10\%$ [18, 24, 28, 29]. From the time evolution of the frequency of the driven and tracked mode, information on parameters other than the AE characteristics themselves, but which depend on them, such as the isotopic mass, or the value of the product $n_e q^2$ (n_e is the electron density) at the Eigenmode resonance location, can also be reconstructed.

3. Summary of low-n linear AE stability studies on JET

The key questions that must be addressed for the stability of ITER burning plasma scenarios are which modes are most unstable, and which parameters control their stability limits [3]. Many magnetic fusion devices can indeed measure the instability thresholds of modes driven by the (anisotropic) fast ions generated by additional heating, with no limitation in toroidal mode numbers other than the diagnostic spatial pass band. However, only the active MHD spectroscopy technique has the capability of evaluating separately the damping of such modes, which is the key unknown in the precise determination of their stability limit. To provide an accurate testing for code predictions, systematic studies are needed to reveal the dependence of the AE damping rate on the (background, fast ions) plasma parameters. It is therefore paramount that the same mode be measured throughout the parameter scan. For this, real-time tracking of the antenna driven modes constitutes in practice an essential tool. For low-n AEs in JET, a large database exists already that satisfies these requirements for comparison with theory, covering a variety of plasma configurations.

Systematic experimental analyses of AE damping rates as a function of the plasma shape and edge magnetic shear were first conducted on JET for radially extended n=1 TAEs and n=0 Global AEs (GAEs) in ohmic limiter discharges [28]. In these discharges, evolving from a limiter to an X-point configuration, the damping rate of the antenna-driven low-n AEs starts relatively low and increases dramatically when the plasma approaches the X-point phase and the edge magnetic shear is increased. As the X-point is formed in the plasma, the damping rate becomes so large ($\gamma/\omega > 5\%$) in ohmic plasmas that in practice the resonance cannot be recognised in real-time any longer. This experimental observation has motivated a significant

amount of theoretical and modelling work [14, 15], and also further experimental measurements for core-localized n=3-10 TAEs driven by resonant ions in limiter and X-point discharges [29]. These comparisons confirm that strong damping can occur for global modes in regions of large magnetic shear at the plasma edge and suggest a strong sensitivity to the edge plasma shape. Such mechanism could be used via appropriate plasma shaping to establish a region free of unstable AEs, where fast ion transport induced by resonant AEs would be prevented. Conversely, modes which are more core-localised, such as EAEs in scenarios with a rather flat q-profile, suffer much less from edge damping mechanisms and maintain a small damping rate, below 1%, even when the edge elongation and magnetic shear are increased towards the values typical of X-point plasmas [30].

In general, although drive and damping mechanisms are qualitatively understood, predictions for the ITER stability necessitate a quantitative knowledge, which can only come from a full validation of codes by dedicated experiments, yet to be completed. In addition to an extreme sensitivity in the theoretical predictions of the damping rates to the details of the plasma equilibrium profiles, several challenges were posed to the theory for damping mechanisms acting in the plasma core for low-n AEs. For example, the model of radiative damping [31] has been demonstrated to be inadequate for low-n TAEs [32], and the role of edge flows [33], of the plasma rotation and its shear [34], and of the plasma beta [35] appear important in the experiment and require a rather comprehensive treatment beyond the MHD model.

Although low-n modes generally appear to be more strongly damped in the experiment than in theoretical predictions, the lack of agreement across the whole range of plasma conditions raises serious doubts on our predictive capabilities for ITER and future reactors. An effort is required on the theoretical side to systematically compare with the data the different models of increasing complexity and identify the necessary ingredients for reproducing the experimental results on the damping. On the experimental side, due to the saddle coil geometry, the medium n=3-15 range could not be explored in JET experiments. As the most unstable modes for ITER are expected to belong to this range [13], and based on the success of the low-n experiments in JET, several experimental groups undertook the challenge to develop new dedicated sets of in-vessel antennas for the excitation and detection of ITER and reactor relevant AEs with intermediate toroidal mode numbers. The different approaches taken in Alcator C-Mod, JET itself, and MAST (in chronological order) are described in the next Sections, along with their main results to date.

4. Alcator C-Mod active MHD system

Alcator C-Mod was the first machine to install and operate active MHD antennas capable of driving medium-n modes for the purpose of exciting stable AEs and measure their damping as a function of plasma conditions [19]. Two antennas were installed in 2002, centred ±17 cm above and below the outboard midplane at one toroidal location. The antennas have 5 rectangular turns and extend 15cm toroidally by 25cm poloidally. Figure 2 shows a picture of the antennas inside the C-Mod vacuum vessel. The antennas are energised by two amplifiers driving up to 25A of current across the frequency range from 100kHz to nearly 1MHz, producing a radial field perturbation of a few Gauss near the q=1.5 surface. The antennas excite a broad toroidal mode spectrum with a full width at half maximum of the order of n~16, which covers the range of mode numbers expected to be unstable in ITER. Given the broad range of excited modes, it is essential to accurately measure the n numbers of the observed resonances in the plasma.

Experiments on C-Mod proved for the first time that intermediate n TAEs can be driven and detected by an antenna system. Resonant n-numbers in the range $3 \leq n \leq 12$ have been observed, with a single dominant mode number, though in many circumstances a clear determination of n is difficult, possibly due to the simultaneous presence of several modes. Measured damping rates are in the range of $0.5\% < \gamma/\omega < 5\%$. Their values and scaling with plasma parameters, for instance with respect to the edge shape, are characterised by significant differences with respect to the low-n regime on JET. Figure 3 shows the measured TAE damping rate for n=6 modes as a function of triangularity [36] indicating at most a small decrease in damping with increasing triangularity, which is in sharp contrast to the strongly increasing damping rate with increasing triangularity for n=1 TAEs on JET [28].

In another experiment, comparing upper and lower single null plasma shapes, the intermediate-n damping rate showed little change with at most a slight increase when the ion ∇B drift direction was toward the X point, as shown in Fig. 4. This result again contrasts the previous results for n=1 TAEs in JET where the damping rate decreased substantially when the ion ∇B drift direction was toward the X point [33]. These results suggest that the damping rate of intermediate-n modes, which are more core-localised than the low-n, more global modes, is less sensitive to changes in the edge conditions than that of low-n modes. This conclusion is consistent with the measurements of the damping rate of EAEs as function of the edge elongation previously performed in JET [30].

Comparisons of the measured damping rate on C-Mod were made with NOVA-K calculations and it was found that good agreement could be obtained within the error bars of the

measurements [37]. However, the results of these comparisons are very sensitive to small changes in the q-profile.

5. The new JET intermediate-n active MHD system

After many years of operation, the JET saddle coil system was dismantled during the 2004-2005 shutdown. To overcome the low toroidal mode number limitation of the saddle coil, a new antenna system was designed and has been installed to replace it and excite modes in the same Alfvén frequency range (20-500kHz). As the ex-vessel excitation system remains essentially the same as that used for the saddle coils, so are the operational capabilities (max. I_{ANT}~30A, max. V_{ANT}~3kV, maximum power ~5kW) [23].

The new antenna comprises two assemblies of four toroidally spaced coils each, situated at opposite toroidal locations. Each coil is made using 18 turns of 4mm Inconel 718 wire (with a static self-inductance of the order of 70μH), covers a toroidal and poloidal extent of ~25cm (hence with NA~1m^2 compared to NA~15m^2 for one saddle coil), and is individually insulated from the supporting frame with Shapal-M spacers. The first turn sits approximately 40mm behind the poloidal limiters. The coils are mounted on a 3mm-thick Inconel 625 open structure, to avoid a closed path for disruption-induced currents. This structure is attached to the poloidal limiters and the remains of the saddle coil brackets through four attachment points. These attachment points are isolated from the frame and the JET vessel with ceramic (Shapal-M) spacers, which are bypassed with 3mΩ resistive straps to provide a known and reliable current path and optimise the mechanical load distribution. The frame and the antennas are further protected by CFC tiles mounted on private mini-limiters. Figure 5 shows the main elements of the antenna design and Fig. 6 shows an in-vessel view of first group of four antennas that was installed in October 2007. The second set of four coils was installed later and became operational for the 2008-2009 campaigns. The AE antennas were almost entirely installed by Remote Handling (RH), through a procedure among the most complex ever undertaken in magnetic fusion devices. Many components and jigs had to be specially designed to comply with the requirements of the RH installation.

Using the pre-existing ex-vessel installation, four modes of active operation are possible: one antenna, two antennas, four antennas and eight antennas, fed by the same amplifier as the saddle coils, through a similar set of distribution and isolation transformers. As for the saddle coils, different antenna phasing combinations (+ and -) can be used. As a result, a spectrum of toroidal mode number covering both the low-n ($n<2$) and medium to high-n range ($n>10$) can be obtained. The “passive” antennas (i.e. those not fed via the amplifier) can be used as

detectors in addition to the magnetic pick-up coils and internal measurements such as ECE and reflectometry. The maximum antenna current and voltage used for the AE excitation experiments to date have been of the order of 10A and 550V, producing a very small antenna-driven magnetic field at the plasma edge, $10^{-6}<|\delta B(G)|<10^{-2}$, as measured with the magnetic pick-up coils. To date, these amplitudes could not be detected clearly enough on the internal fluctuation measurements, even using synchronous detection, to allow unambiguous internal mode structure reconstruction. The control of the exciter frequency and the resonance detection algorithms are essentially identical to those used for the saddle coils, described above in Section 2. The only notable difference is that now the synchronously detected data for eight different (and user-selectable) pick-up coils are acquired in real-time, hence allowing discrimination between low-n and medium to high-n modes.

The vacuum spectra that can be obtained with four or eight active antennas are shown in Fig. 7, to represent the operational capabilities with one and two coil sets. The excited n-spectrum extends up to n>20 and is clearly purer and more "localised" in n-space by combining toroidally opposite antennas. Code calculations also demonstrate that this arrangement provides a coupling to the plasma for a n=5 Toroidal AEs (TAE) that is of the same order as that achieved with the saddle coils for an n=2 TAE for the same JET equilibrium.

Damping rate data were obtained for more than 2000 discharges, with real-time tracking of the driven plasma resonance on about a third of these, covering different JET operating regimes. The n-spectrum that can be excited in the plasma by the new antennas extends up to n~20 also in X-point configurations.

Real-time mode tracking has been obtained for all antenna excitation configurations in a large variety of plasma regimes (in limiter and X-point), up to moderate heating power (P_{NBI}<6MW). At higher P_{NBI}, background broadband turbulence dominates the synchronously detected signals and usually prevents a clear detection of the modes using the edge pick-up coils, particularly for those with medium to high toroidal mode number (n>5).

Measurements of the damping rate for low- and medium-n AEs have been obtained for various JET operating regimes, with real-time tracking of the driven resonances providing tens of individual damping rate data on a single discharge. We present here three examples of quantitative measurements of the damping rate for low- and medium- to high-n AEs.

Given the extension of the antenna excitation toroidal mode number spectrum, it is difficult to separate the different toroidal harmonics and evaluate the frequency, mode number and damping for each one of them using simple tools such as linear phase fitting of the residue amplitudes [24]. Various numerical tools were then assessed to resolve the uncertainty in the

n-number determination, including the Discrete Fourier Transform, Singular Value Decomposition and the Lomb Periodogram. The use of all these tools is also further complicated by the limited number of (unevenly distributed) pick-up coils available to cover the toroidal cross-section. Finally, the *Sparse Spectrum* technique [38, 39], as developed in the *SparSpec* code (freely available at http://www.ast.obs-mip.fr/Softwares) was found to be able to reproduce very satisfactorily a simulated spectrum of AE data on JET [40]. The *SparSpec* code has been previously only used for the analysis of astrophysical data and has now being fully adapted for routine use on JET data, including real-time applications. The *SparSpec* method is based on the principle of sparse representation of signals, where sinusoids are fitted to irregularly sampled data. The model used in *SparSpec* is linear in the fitting parameter (toroidal mode numbers in our case, temporal frequencies in astrophysics): the data is modelled as a large number (possibly larger than the data size) of pure modes, discretized on a fixed, arbitrarily thin grid, and only their amplitudes need to be estimated. Among the many representations fitting the data, the one with the fewest non-zero amplitude is sought, i.e. the sparse spectrum.

The first, essential verification of the experimental measurements obtained with the new antennas is the capability of driving and tracking in real-time modes that can unambiguously be identified as AEs. This is best done by setting the antenna operating frequency to the EAE range, for which the mode frequency is twice that of TAEs, $f_{EAE} \sim 2 \times f_{TAE}$, as this frequency range is in fact essentially free from other instabilities driven by plasma background parameters (such as Drift-Kinetic Alfvén Waves, Geodesic Acoustic Modes or Neoclassical Tearing Modes), at least in the absence of fast ions. Figure 8a shows that the Alfvénic nature of the modes being tracked by the AELM is demonstrated unambiguously by considering the case of EAEs, and Fig. 8b shows the measured mode frequencies, damping rate for all the mode numbers inferred in the detected spectrum using the *SparSpec* code. Note that in this case the strongest coupling occurs for a n=0 GAE. Even in the absence of clear internal fluctuation measurements, an analysis of the absolute value of the frequency of these modes, and of its scaling with the plasma density and magnetic field excludes the possibility that these are just antenna driven edge fluctuations.

Given the rather different excitation spectrum obtained with the new antennas compared to that obtained with the old saddle coils, it is also essential to verify that the damping rate of low-n modes (i.e. the same as driven by the saddle coils) measured with the new antennas is the same in the same experimental conditions of the saddle coil measurements, namely ohmic limiter discharges with low edge elongation ($\kappa_{95} \sim 1.3$) and triangularity ($\delta \sim 0.1$). Figure 9

shows that in these experimental conditions the damping rate of n=0 GAEs, as measured with the new antennas (using the excitation spectrum ++++) is essentially identical to that measured with the old saddle coils [24, 28]. Note that the n=10 mode appearing in the spectrum is in this case an artefact of the *SparSpec* decomposition in toroidal components.

These two experimental results clearly demonstrate that the new antenna system has the same technical and scientific capabilities of the old saddle coil system for low-n modes, and at the same time illustrate the complexity of the n-spectrum being driven by such compact and toroidally localised antennas. Many components clearly coexist in the spectrum, even for the simplest ++++ phasing configuration, hence the necessity to develop and test very reliable methods to confidently separate these different toroidal harmonics in the spectrum of fluctuations detected, for instance, by the edge pick-up coils. This has now been fully accomplished by implementing the *SparSpec* code in real-time on JET. Moreover, when using excitation configurations that drive a wider and a higher n-spectrum (|n|~5-20), one has to cope as well with the much lower antenna-driven B-field which is achieved at the plasma edge. For each component we have in fact $|\delta B| \sim 1 \times 10^{-5}$G with the +-+- phasing compared to $|\delta B| \sim 3 \times 10^{-4}$G for the ++++ phasing. This can be further complicated by the presence of a much larger background turbulence and greater antenna-plasma distance when searching for these modes in X-point configurations in the presence of high power additional heating, such as Ion Cyclotron Resonance Frequency (ICRF) and/or Neutral Beam Injection (NBI). These difficulties are also experienced in the C-Mod experiments, as discussed in Section 4. In this respect, routine availability of internal measurements (via ECE and reflectometry, for instance) may prove very useful, if combined with improved coupling due to a better antenna impedance matching, in helping to detect the different higher-n components, as these modes are more core-localized than the lower-n modes and are therefore expected to be detected more easily with these diagnostics than with the edge pick-up coils.

Figure 10 illustrates the measurement of the damping rate in plasmas in X-point configuration during the additional heating phase of a discharge in the conventional tokamak scenario, i.e. with a monotonic q–profile with $q_0 \sim 1$. In this plasma scenario the antenna-plasma distance, as evaluated by the ROG (radius of outer gap) parameter is of the order of ROG~15cm compared to the much lower ROG~8cm for the typical plasmas in limiter configuration. The antenna excitation spectrum was ++++, driving predominantly low-n modes. For the n=0 mode being tracked during the ICRF heating phase, we note that at the ICRF power switch-off (t>14sec) the total damping rate increases, which suggests a reduction in the fast ion drive

to the total damping of the stable modes. Other harmonics with higher n's are being detected outside the tracking phase.

Figure 11 shows two examples of mode frequency and damping rate data obtained using the +-+- antenna excitation spectrum for plasmas in X-point configuration during the ohmic and high-power additional heating phase, P_{NBI}~10MW and P_{ICRF}~4MW. In both cases the q-profile is monotonic with q_0~1, and the antenna-plasma distance is ROG~12cm. No fast ion driven instabilities are observed in these discharges. In #69661 the magnetic field ripple has the standard value of 0.1% (obtained with 32 toroidal coils), whereas for #69663 the B-field ripple is 0.65% (obtained using 16 toroidal coils). The decomposition in toroidal components performed with the *SparSpec* code indicates that rather high-n modes are present, which is consistent with the +-+- antenna excitation spectrum, but most of the components with $|n|>10$ have a very small relative amplitude (as measured with magnetic pick-up coils at the plasma edge) compared to the $|n|<5$ components. Typically, their ratio is of the order of $|\delta B(|n|>10)|/|\delta B(|n|<5)|\sim 0.05$, which in turn corresponds to absolute values of $|\delta B|$ very close to the background noise level and the hardware detection limit, $|\delta B|\sim 10^{-6}$G. In the case of a larger B-field ripple, modes with $|n|$~5-15 appear to have a larger damping rate during the additional heating phase than in the case of standard ripple, whereas in the ohmic phase the damping rate are similar for both values of the B-field ripple. These results are interesting as they not only indicate that a large number of modes with relatively low damping rate ($\gamma/\omega<1\%$) and covering a wide range in toroidal mode numbers can exist in the presence of strong additional heating (P_{NBI}~10MW leading to β_N~1), but also that the mode stability is affected by the B-field ripple, either directly or via a reduction in the fast ion drive, possibly through orbit redistribution.

6. MAST active MHD system

In contrast to conventional aspect-ratio devices, spherical tokamaks (STs) such as MAST with their low toroidal magnetic field, typically inject super-Alfvénic neutral beam ions providing the possibility of studying fast particle instabilities that are strongly driven by their primary resonance ($\upsilon=\upsilon_A$). Furthermore, data from high β operation on both MAST and START has suggested that as $\beta_{thermal}$ increases, the core Alfvén instabilities weaken, and both the mode amplitude and number of unstable modes are reduced. An alternative and complementary method of studying Alfvén Eigenmodes is to use an external antenna to excite the modes and

to study their properties whilst still stable. This also allows one to directly distinguish between AEs and EPMs.

To this aim, the first three coils of a new active AE antenna array, out of a full array of 12 coils, have been installed on MAST in 2006 [21]. These coils are below the machine midplane with a relative toroidal position of 0°, 60° and 180°. The final system, shared with other physics activities, including ELM control, encompasses 6 coils below the midplane and 12 above. Each coil is of a four turn rectangular pancake 600mm long by 270mm, made from 20×9mm aluminium conductor with a separation between conductors of 4mm. The coil is fed by an aluminium coaxial feed, with an additional bellows and steel tube cover to protect the feed from the plasma. The primary electrical insulation up to 3kV for the coil is a 20μm thick Al_2O ceramic coating. The advantage of this coating is high hardness and high wear resistance. It is flexible, forming a good bond with the substrate, can withstand temperatures up to 2000^0C and is highly resistant to thermal shock. For plasma protection and additional electrical isolation, the whole coil is encased in a 15mm thick Boron Nitride shell. This cover is then painted externally with colloidal graphite to reduce reflections which would affect visible imaging diagnostics. The coils are mounted using brackets attached to the lower poloidal field coil. An image of one of the MAST coils is shown in Fig. 12a, whereas Fig. 12b illustrates the position of the full set of antennas in the MAST vacuum vessel.

Each coil is powered individually by a 500W power amplifier. To match the TAE coil to the power supply, a matching circuit is fitted at the coil feed-through. This constitutes a significant advantage with respect for example to the JET case, where the matching unit can only be on the amplifier side of the transmission line, i.e. about 100m away from the in-vessel antennas. Tests using a network analyzer show a good match between load and amplifier with the load impedance remaining in the range 48-51Ω over a wide frequency range (50-700kHz), with reflected power fractions not exceeding 10% even in the presence of plasma.

The toroidal mode number spectrum, with two coils at 0° and 180°, contains either entirely odd or even modes depending on the relative phase of the current in the two coils. With the currents in phase the predominant mode is n=2, out of phase it is n=1. On the detection side, a large number of Mirnov coils are already available on MAST, measuring fluctuations in the range 100kHz-4MHz and capable in principle of determining mode numbers up to n = 20.

Initial experiments have been performed using two coils in n=1 configuration. The drive frequency was swept with 50ms linear ramps up and down between 75kHz and 175kHz. A clear increase (by an order of magnitude) in the strength of the (digitally) synchronously detected Mirnov coil signal was observed in the presence of plasma. Cross-over distortion due

to the amplifier was observed to cause harmonic generation. Figure 13 shows an example of a magnetic spectrogram with the MAST active AE antenna system sweeping in frequency from 85kHz to 180 kHz. As can be clearly seen from the plasma response there is a weakly damped mode excited by the antenna at around 65ms and a strongly damped mode at around 120ms.

As the frequency was swept across the calculated TAE and NAE gap range, several resonances were detected [41]. An example of a resonance in the antenna-plasma transfer function, fitted to extract a damping rate, is shown in Fig. 14. Although a complete identification of these resonances as AEs, and a reconstruction of the mode numbers and structure are still missing, the damping rate of these modes was determined using the same technique described in Section 2. These initial experiments indicate very large damping rates in the range γ/ω~4%-20%. A systematic identification of the observed resonances and a study of dependence of the damping rates with the plasma β are to be undertaken soon.

7. Conclusions and outlook

The basic physics principles of the linear physics of Alfvén Eigenmodes can be considered essentially understood, following a significant effort in experimentation and theoretical modelling. The fast ion physics community is getting quite close to a complete definition of stability properties of modes prone to resonant interaction with fast ions in ITER. However, despite large data sets of AE instability thresholds in the presence of different classes of fast ions, and of damping rates for stable, antenna driven AEs on JET and Alcator C-Mod, no conclusive benchmarking exists for the models to be used for predicting the stability of ITER plasmas with respect to fast ion (α) driven modes. Such prediction is essential in the preparation of scenarios, both for machine safety and for an optimisation of the fusion burn.

To complete such challenge it will be necessary to take advantage of the recently improved core fluctuation diagnostics for the internal mode structure reconstruction, and of the recently developed active MHD tools (in particular for the ITER and reactor relevant intermediate-n regime) to establish a database with all adequate information for providing stringent tests for the theoretical modelling of AE stability in ITER, DEMO and future reactors.

On the theoretical side, codes need to be completed to account for all possible damping mechanisms and improve quantitative predictions, following systematic comparisons with data, in particular in regimes in which several modes can be present. Such regimes present difficulties in the comparison, which are representative of what will be encountered in ITER. For example, it will be practically necessary to know not only the frequency and poloidal and

toroidal structure of a mode to identify it theoretically and assess its damping and drive, but also its internal (radial) eigenfunction shape, which imposes a clear requirement for core diagnostics with adequate temporal and spatial resolution. In addition, methods to quantify the degree of agreement between theory and experiments need to be devised, to quantify the confidence interval for ITER predictions. Another important aspect to be implemented in numerical codes for reliable extrapolations to ITER is the modelling of a realistic plasma boundary, characterized by X-point geometry and the presence of a scrape off layer, as for instance those preliminary considered in [42] in an *ad-hoc* way.

The comparison of experimental results with state-of-the-art codes for stability predictions is being undertaken much more systematically than in the past, starting with a few reference cases (high and low-n) for drive and damping of AEs in ITER relevant plasma scenarios on JET. Such comparisons are being established for single modes and will be extended to cases with several modes. The effect of plasma shape and parameters on AE damping will be assessed, for example comparing similar scenarios with open or closed Alfvén gap structure. In addition, they should be complemented by studies of the sensitivity of the results with respect to small variations in the plasma configuration and parameters, to quantify the credibility of the theoretical predictions. Only through a complete assessment of the stability of the known AEs in the known regimes will one be able to observe and interpret possible unexpected results that may come from different wave-particle interaction regimes brought about in future burning plasmas by a different parameter range from present devices, in particular in terms of the value of the ratio of the fast ion orbit sizes to the device size.

Following the low-n active MHD experiments on JET using the saddle coils, C-Mod first, the new antenna system at JET then, and finally MAST, have all shown that excitation of AEs using localised antenna structures is possible. Experiments on C-Mod have shown that external AE excitation is possible in high field, high density and $T_e \sim T_i$ regimes, while results obtained using the new eight-coil antenna on JET confirm that excitation is possible in a large volume plasma, together with real time tracking of core modes throughout the limiter and X-point phases of high performance discharges, with significant additional heating. This result was obtained using compact antennas with a small effective area and located rather away from the plasma edge, which is a very promising technical result in view of a possible use of compact active antennas in ITER for burn control applications [43]. MAST has proven that stable AEs can be launched and detected also in a tight aspect ration device, and, more importantly, in high β plasmas.

Experimentally, a number of problems that have been identified as common to the active MHD antenna systems need to be addressed. First, coupling and mode selectivity should be improved, for instance using independent amplifiers for each antenna and imposing an arbitrary antenna-to-antenna phasing. In C-Mod, conditions in which the mode number of the driven AE does not vary throughout the discharge need to be identified and obtained reproducibly. When MAST will eventually be obtaining data with the full set of antennas, mode selectivity is not expected to be a problem. A possibility on all devices is to perform experiments in the presence of a significant toroidal plasma rotation, in which resonances corresponding to different mode numbers would naturally appear separate in the laboratory frame due to the Doppler effect.

On the detection side, internal measurements of the AE spectrum need to become more reliable and routinely available, hence providing further insight for determining the radial mode structure. These measurements are of paramount importance not only for confirming that localised antennas do indeed drive core modes, but also for the definition of a stringent framework for the experiment-to-theory comparison. As clearly demonstrated in JET, the medium-n range is far richer in Alfvénic resonances which can all be simultaneously present in the plasma. Furthermore, the availability of internal measurements will be particularly useful for medium-n, core-localised modes, for which the mode amplitude measured with magnetic pick-up coils at the plasma edge is often very close to the background noise level, compromising the quality of the ensuing data analysis.

Finally, active MHD experiments on all devices should explore the possibility of performing a controlled fast ion redistribution experiment, in which the external signal is used in a controlled fashion to affect the spatial distribution of the fast ions that resonate with the driven modes. Such an experiment would have an impact well beyond the physics of the mode linear stability, as it would provide a test for the nonlinear wave-particle interaction models, and a quantitative benchmark for the fast ion transport codes [44-46].

This work has been conducted under the European Fusion Development Agreement. The views and opinions expressed herein do not necessarily reflect those of the European Commission. A.Fasoli and D.Testa were partly by the European Communities under the contract of Association between EURATOM and CRPP. J.Snipes, A.Klein and J.Sears were partly supported by the DoE contracts No. DE-FG02-99ER54563 and DE-FC02-99ED54512. M.Gryaznevich, R.Martin and S.Pinches were partly funded by the United Kingdom

Engineering and Physical Sciences Research Council and by the European Communities under the contract of Association between EURATOM and UKAEA.

References

1) M.N.Rosenbluth and P.H.Rutherford, Phys. Rev. Lett. **34** (1975), 1428.
2) C.Z.Cheng, L.Chen and M.S.Chance Ann. Phys., NY **161** (1985), 21.
3) A.Fasoli et al. Nuclear Fusion **47**, (2007), S264.
4) H.L.Berk, J.W.Van Dam, Z.Guo and D.M.Lindberg, Phys. Fluids **B4** (1992), 1806.
5) F.Zonca and L.Chen, Phys. Rev. Lett. **68** (1992), 592.
6) R.Mett and S.M.Mahajan, Phys. Fluids **B4**, (1992), 2885.
7) N.N.Gorelenkov and S.E.Sharapov, Physica Scripta, **45**, (1992), 163.
8) R.Betti and J.P.Freidberg, Phys. Fluids **B4** (1992), 1465.
9) A.B.Mikhailovskii, Sov. Phys. JETP **41** (1975), 890.
10) M.A.Van Zeeland et al., Phys. Rev. Lett. **97** (2006), 135001.
11) W.W.Heidbrink et al., Phys. Rev. Lett. **99** (2007), 245002.
12) M. García-Muñoz et al., Phys. Rev. Lett. **100** (2008), 055005.
13) W.Heidbrink et al., Plasma Phys. Control. Fusion **45** (2003), 983.
14) A.Fasoli, A.Jaun, D.Testa, Phys. Lett. **A265** (2000), 288.
15) A.Jaun, A.Fasoli, J.Vaclavik, L.Villard, Nucl. Fusion **40** (2000), 1343.
16) D.Borba et al., Nucl. Fusion **42** (2002), 1028.
17) A.Jaun, A.Fasoli, D.Testa, J.Vaclavik, L.Villard, Plasma Phys. Control. Fusion **43** (2001), 207.
18) A.Fasoli et al., Plasma Phys. Control. Fusion **44** (2002), 159.
19) J.A.Snipes, D.Schmittdiel, A.Fasoli, R.S.Granetz, R.R.Parker, Plasma Phys. Cont. Fusion **46** (2004), 611.
20) D.Testa et al., Proceedings of the 23rd Symposium on Fusion Technology (SOFT), Venice (Italy), 20-24 September 2004.
21) R.Martin et al., Proceedings 34th EPS Conference on Controlled Fusion and Plasma Physics, Warsaw (Poland), 02 – 06 July-2007.
22) G.Matsunaga et al., Proceedings of 10th IAEA Technical Meeting on Energetic Particles in Magnetic Confinement Systems, Kloster Seeon, Germany, 2007.
23) A.Santagiustina et al., Proceedings of the 19th Symposium on Fusion Technology, Lisbon, 16-20 September 1996, vol.1, p.989.
24) A.Fasoli et al., Phys. Rev. Lett. **75** (1995), 645.
25) C.Boswell, private communication, JET 2005.
26) A.Fasoli et al., Proceedings XV IAEA International Conference on Plasma Physics and Controlled Fusion, Sevilla (Spain), 1994.

27) L.Villard, J.Vaclavik, Nucl. Fusion **37** (1997), 351.
28) D.Testa, A.Fasoli, Nuclear Fusion **41** (2001), 809.
29) D.Testa et al., Plasma Phys. Control. Fusion **46** (2004), S59.
30) C.Boswell, A.Fasoli, J.A.Snipes, D.Testa, Proceedings 47th Annual Meeting of APS Division of Plasma Physics, Denver (USA), 24-29 October 2005.
31) G.Y.Fu et al., Phys. Plasmas **3** (1996), 4036.
32) D.Testa, G.Y.Fu, A.Jaun, A.Fasoli, O.Sauter, Nucl. Fusion **43** (2003), 479.
33) D.Testa, A.Fasoli, C.Boswell, Nucl. Fusion **46** (2006) 829.
34) D.Testa, C.Boswell, A.Fasoli, Nucl. Fusion **45** (2005), 907.
35) D.Testa, A.Fasoli, A.Jaun, Nucl. Fusion **43** (2003), 724.
36) J.A.Snipes, N.Basse, C.Boswell, E.Edlund, A.Fasoli, Phys. Plasmas **12** (2005), 056102.
37) J.A.Snipes, N.N.Gorelenkov, J.A.Sears, Nucl. Fusion **46** (2006), 1036.
38) S.Bourguignon, H.Carfantan, T.Bohm, Astronomy and Astrophysics **462** (2007), 379.
39) S.Bourguignon, H.Carfantan, J.Idier, IEEE Selected Topics in Sig. Proc. **1** (2007), 4.
40) A.Klein, H.Carfantan, D.Testa, et al., Plasma Phys. Control. Fusion **50** (2008), 125005.
41) S.Pinches et al., Proceedings of 10th IAEA Technical Meeting on Energetic Particles in Magnetic Confinement Systems, Kloster Seeon, Germany, 2007.
42) G.Y.Fu, H.J.Berk, A.Pletzer, Phys. Plasma **12** (2005), 082505.
43) A.Murari et al., Plasma Phys. Control. Fusion **47** (2005), B249.
44) G.Vlad, S.Briguglio, G.Fogaccia, F.Zonca. M.Schneider, Nucl. Fusion **46** (2006), 1.
45) F.Zonca, S.Briguglio, L.Chen, G.Fogaccia, G.Vlad, Nucl. Fusion **45** (2005), 477.
46) F.Zonca, L.Chen, Plasma Phys. Control. Fusion **48** (2006), 537.

Figure Captions

Figure 1. AE resonance seen in the antenna loading, as measured at two different points along the power transmission line: at the Distribution Unit output (label: DU), located about 80m before the antenna (long coaxial cable), and at the limb junction box (label: LJB), located much closer to the antenna, about 10m before the feedthrough. The antenna loading is shown for clarity only for one saddle coil (SC3L), with very similar results for the other active antenna (SC7L). Note that the antenna loading increases at the DU and decreases at the LJB when a resonance is found in the plasma.

Figure 2. The C-Mod antennas and their position inside the vacuum vessel at a single poloidal and toroidal location.

Figure 3. The measured TAE damping rate for n=6 modes as a function of average triangularity in the C-Mod tokamak. The plasma equilibria for the two extreme cases in the scan are also shown.

Figure 4. Measurement of the TAE damping rate as function of the ∇B-drift direction in C-Mod for medium-n modes. The two corresponding plasma equilibria are also illustrated.

Figure 5. New JET intermediate-n antennas: engineering layout of one group of four coils, showing the main components.

Figure 6. New JET intermediate-n antennas: front view of one group of four coils as installed in-vessel in October 2007. The second antenna frame is also installed in the toroidally opposite location at the same poloidal angle.

Figure 7. New JET intermediate-n antennas: examples of the calculated vacuum excitation spectra using four or eight antennas. Note that with eight antennas the n-number spectrum is much purer and more "localised".

Figure 8a. Tracking in real-time of a mode in the EAE frequency range for JET discharge #69587, unambiguously showing the Alfvénic nature of the instabilities driven with the new antenna system. The magenta line, used for scaling purposes, corresponds to the initial guess for the EAE frequency used for the real time algorithm, and is evaluated at the center of the n=1 EAE gap and assuming q=1.5.

Figure 8b. Frequency and damping rate for the different components of the n-spectrum driven and detected by the new JET antenna system for the modes shown in Fig9a, as evaluated using the SparSpec code. The antenna excitation spectrum was ++++, giving a dominant n=0 harmonic (about 85% of the power spectrum) when the mode is being tracked, with other harmonics appearing when the real-time tracking is lost between t=29.2sec and t=30.5sec.

Figure 9. Mode frequency, damping rate and background plasma parameter for an ohmic limiter JET discharge where the four antennas were excited in the ++++ phasing configuration. The dominant harmonic in the driven and detected n-spectrum is the n=0 mode, with the n=10 mode most likely being an artefact of the SparSpec decomposition in toroidal harmonics. For the n=0 AE, the damping rate measured with the new antennas is essentially identical to that obtained with the old saddle coils in very similar experimental conditions. The labels BTOR and HRES indicate the synchronously detected signal measured at different magnetic pick-up coils (in arbitrary units).

Figure 10. Mode frequency, damping rate and background plasma parameter during the additional heating phase (P_{NBI}~4MW, P_{RF}~1.5MW) of an X-point JET discharge with monotonic q-profile, with ROG~15cm and q_0~1. The antenna configuration spectrum was ++++, driving predominantly low-n modes. For the n=0 mode being tracked during the ICRF heating phase, we note that at the ICRF power switch-off (t>14sec) the damping rate increases, thus indicating a reduction in the fast ion drive. Other harmonics with higher n's are being detected outside the tracking phase.

Figure 11. Mode frequency and damping rate for standard and high B-field ripple (01% and 0.65%, respectively), in two X-point JET discharges during the ohmic and high-power additional heating phase (P_{NBI}~10MW, P_{RF}~4MW and β_N~1). A larger γ/ω>2% is found during the NBI heating phase with the higher B-field ripple, whereas similar damping rates are obtained during the ohmic phase. Note that the measurements for modes with |n|>10 may be compromised by their amplitude being very close to the background noise level.

Figure 12a. One of the new active MAST AE antennas, installed in-vessel.

Figure 12b. A schematic view of the interior of MAST, showing the in-vessel position of the active AE antennas. The yellow antennas in the figure are those used in the initial trial installation, and correspond to those used in generating the results shown in Fig. 14.

Figure 13. Magnetic spectrogram for MAST #18487 showing active AE diagnostic sweeping in frequency from 85kHz to 180kHz and exciting a weakly damped mode at around 65ms and a strongly damped mode at around 120ms. The overlaid white lines approximately indicate the frequency range around which TAE modes and EAE modes may be expected to be excited.

Figure 14. First data from MAST using the newly installed antennas: measured (solid lines) and fitted (dotted lines) transfer functions for two toroidally separated magnetic pick-up coils for MAST #18487. A clear resonance is observed at 148.9kHz (indicated by the vertical dot-dash lines) with damping rate γ/ω=4.15%, but the toroidal mode number was not identified.

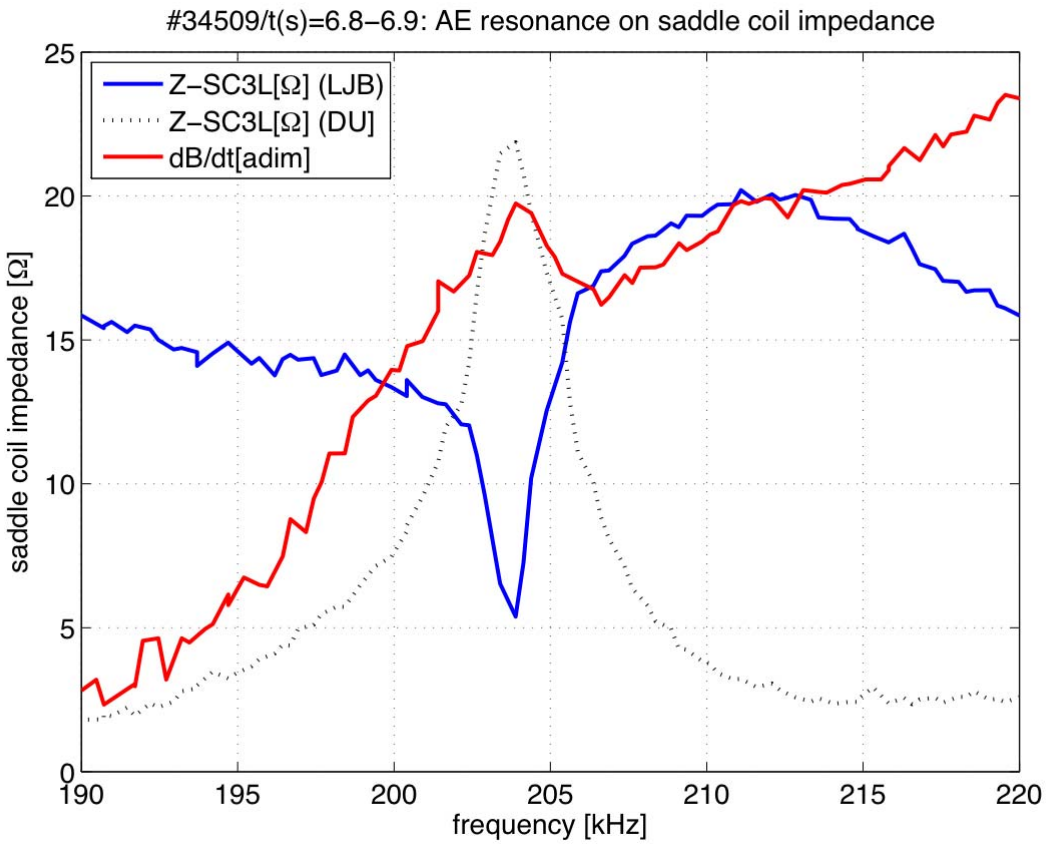

Figure 1. AE resonance seen in the antenna loading, as measured at two different points along the power transmission line: at the Distribution Unit output (label: DU), located about 80m before the antenna (long coaxial cable), and at the limb junction box (label: LJB), located much closer to the antenna, about 10m before the feedthrough. The antenna loading is shown for clarity only for one saddle coil (SC3L), with very similar results for the other active antenna (SC7L). Note that the antenna loading increases at the DU and decreases at the LJB when a resonance is found in the plasma.

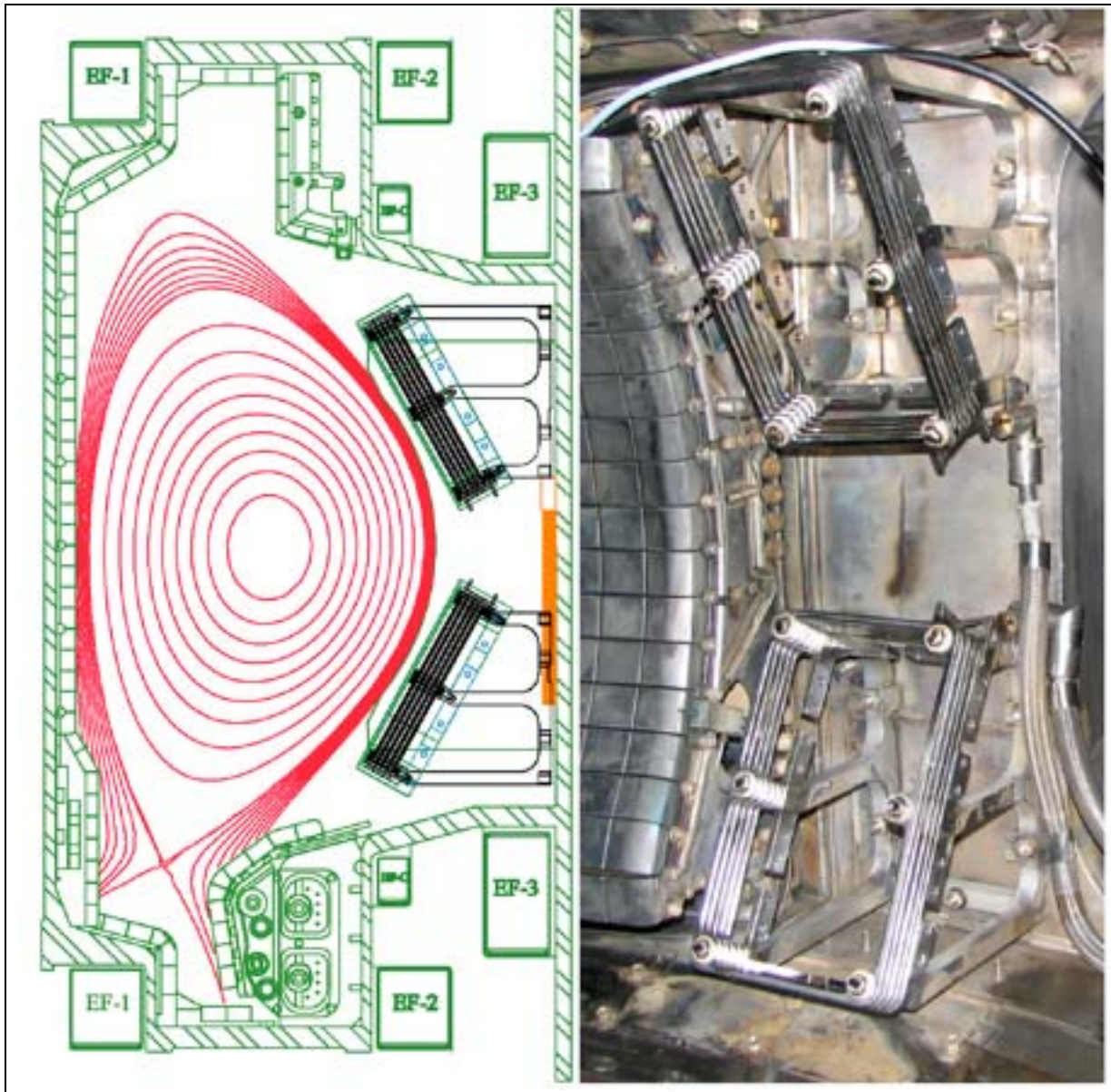

Figure 2. The C-Mod antennas and their position inside the vacuum vessel at a single poloidal and toroidal location.

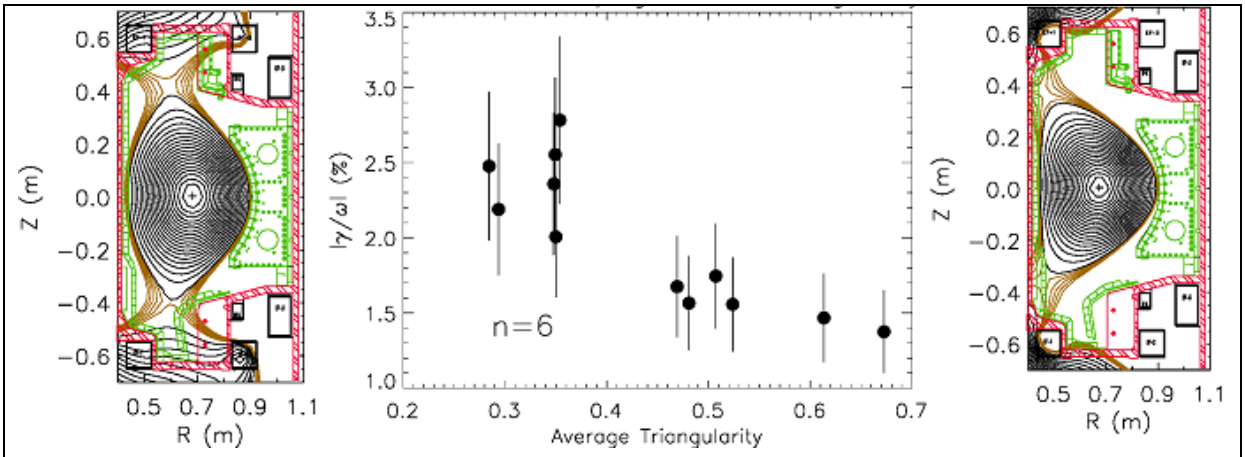

Figure 3. The measured TAE damping rate for n=6 modes as a function of average triangularity in the C-Mod tokamak. The plasma equilibria for the two extreme cases in the scan are also shown.

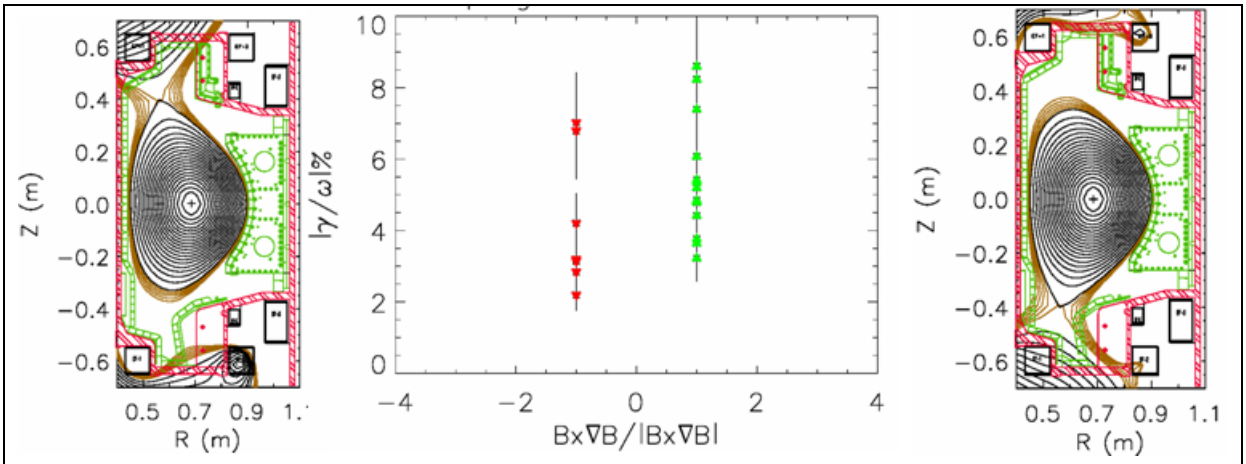

Figure 4. Measurement of the TAE damping rate as function of the ∇B-drift direction in C-Mod for medium-n modes. The two corresponding plasma equilibria are also illustrated.

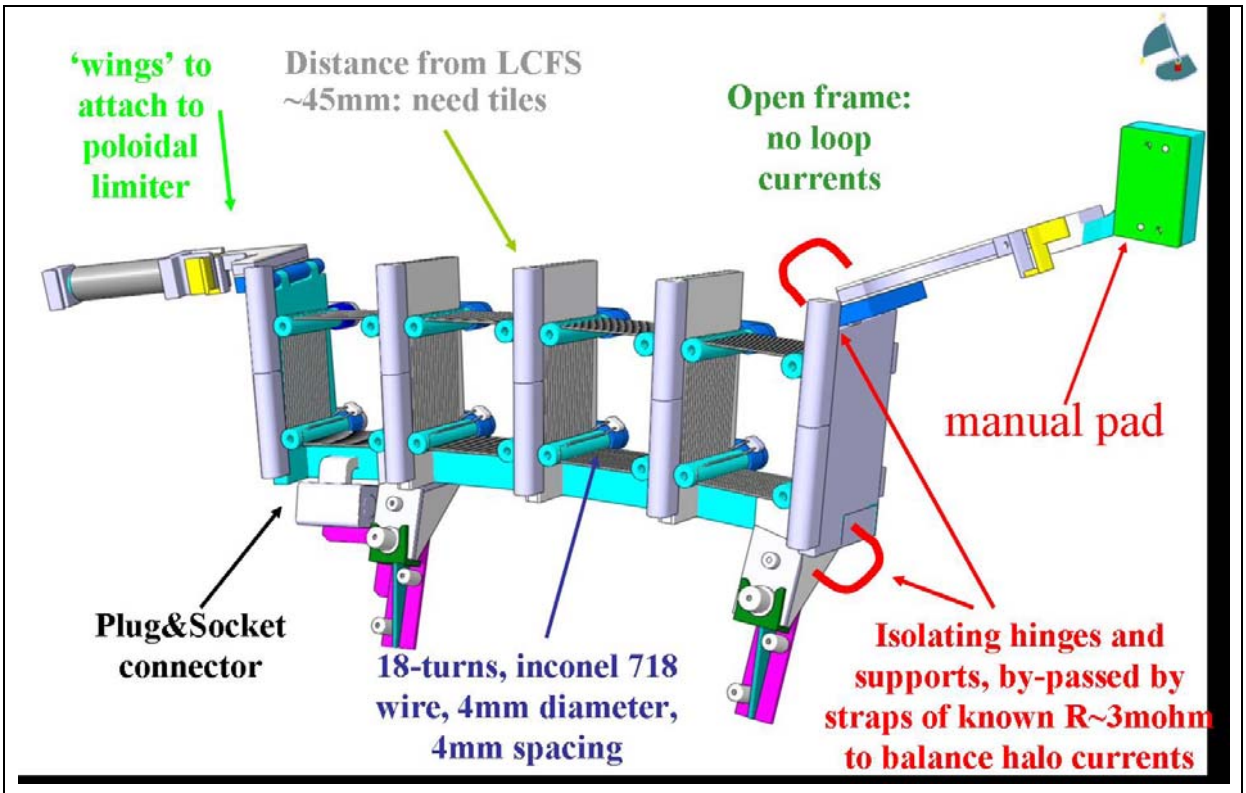

Figure 5. New JET intermediate-n antennas: engineering layout of one group of four coils, showing the main components.

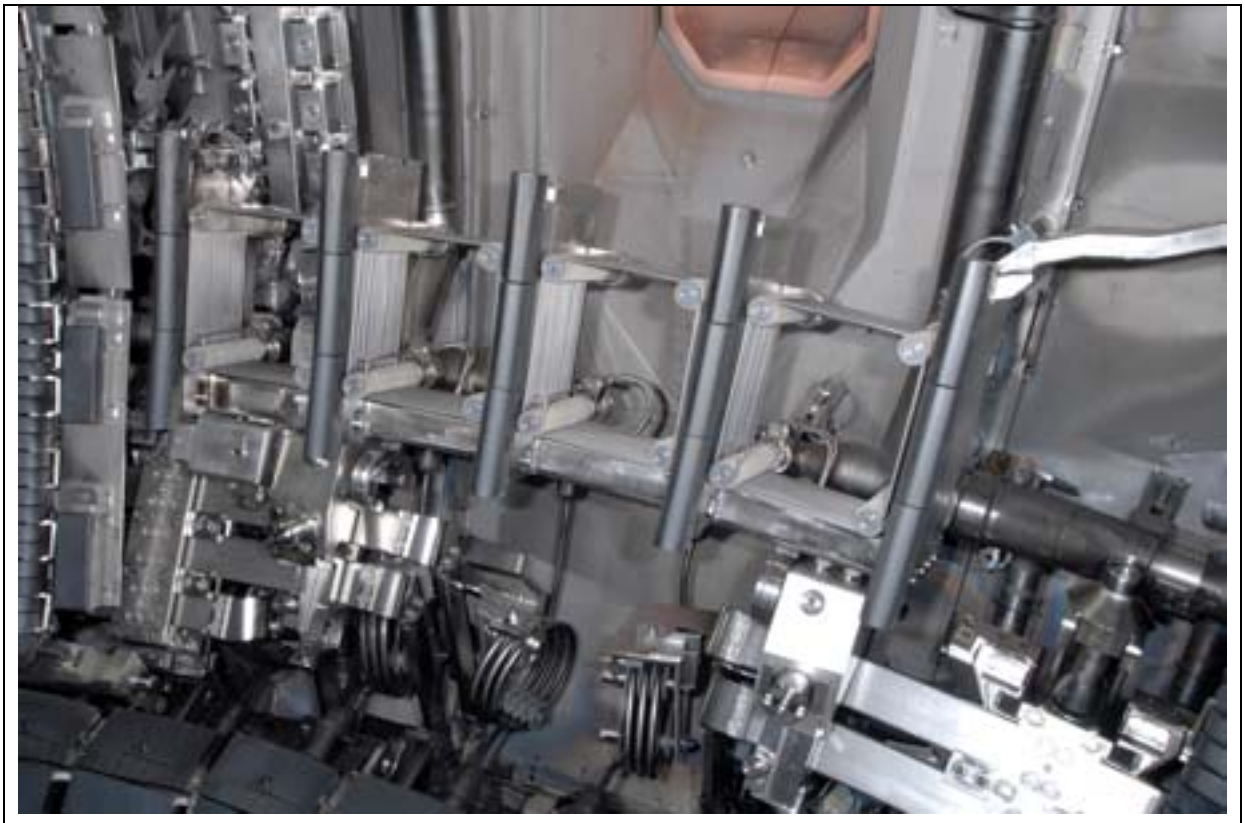

Figure 6. New JET intermediate-n antennas: front view of one group of four coils as installed in-vessel in October 2007. The second antenna frame is also installed in the toroidally opposite location at the same poloidal angle.

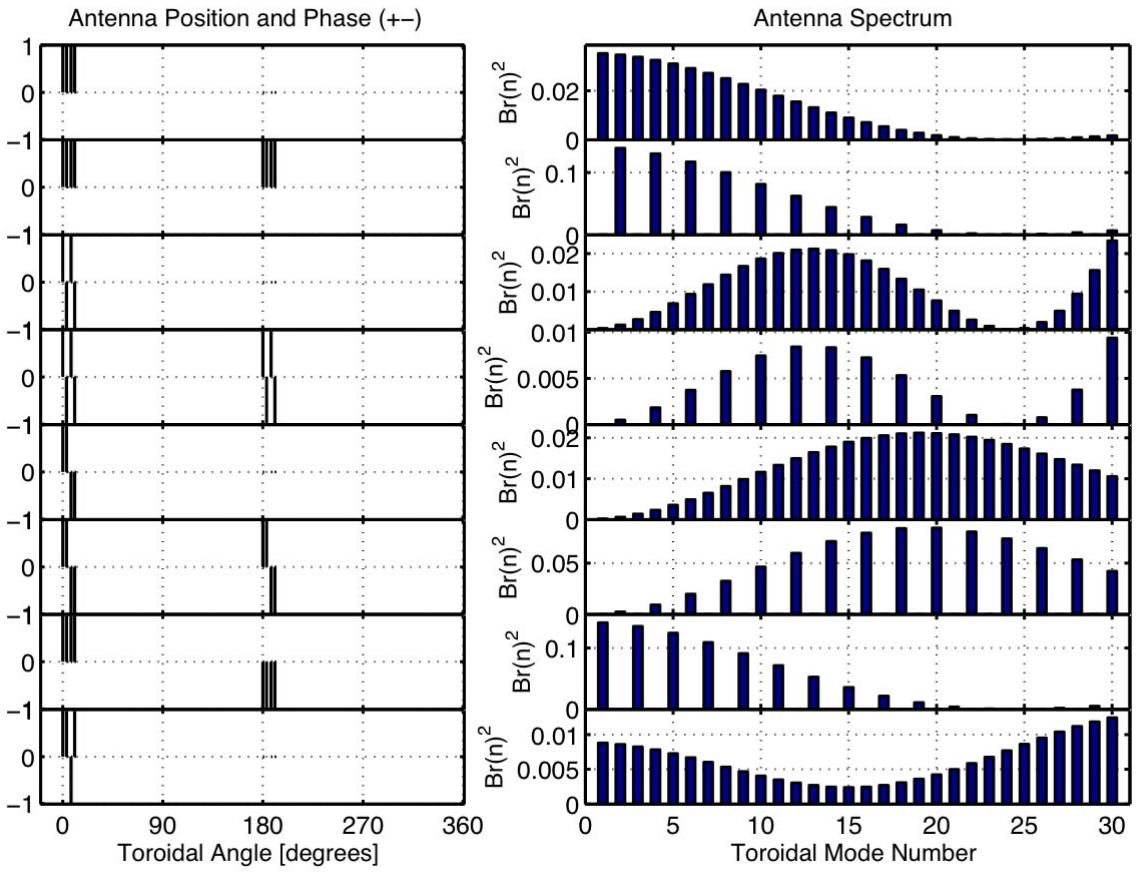

Figure 7. New JET intermediate-n antennas: examples of the calculated vacuum excitation spectra using four or eight antennas. Note that with eight antennas the n-number spectrum is much purer and more "localised".

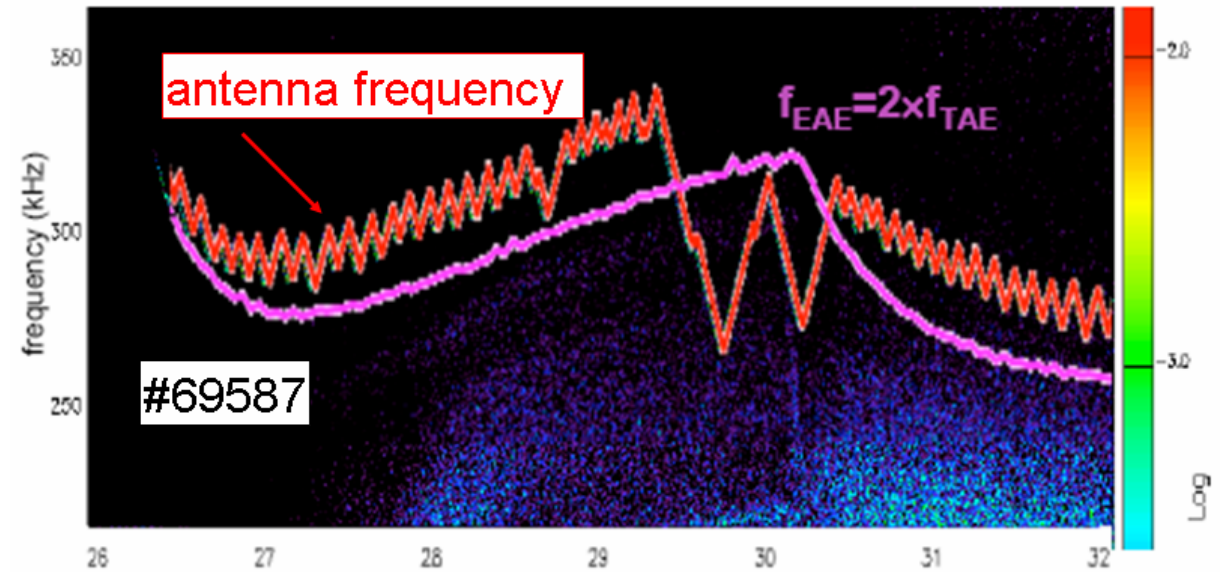

Figure 8a. Tracking in real-time of a mode in the EAE frequency range for JET discharge #69587, unambiguously showing the Alfvénic nature of the instabilities driven with the new antenna system. The magenta line, used for scaling purposes, corresponds to the initial guess for the EAE frequency used for the real time algorithm, and is evaluated at the center of the n=1 EAE gap and assuming q=1.5.

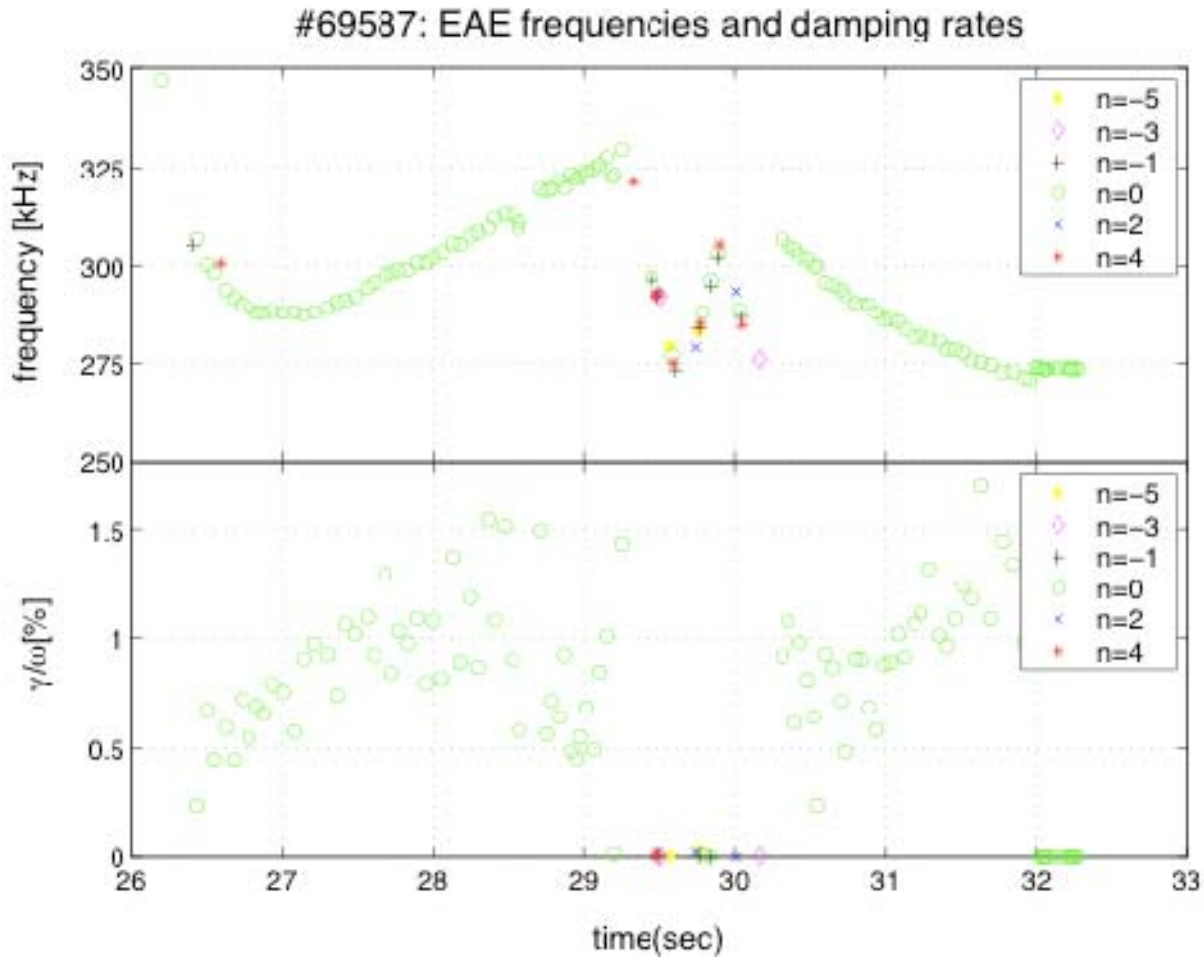

Figure 8b. Frequency and damping rate for the different components of the n-spectrum driven and detected by the new JET antenna system for the modes shown in Fig9a, as evaluated using the SparSpec code. The antenna excitation spectrum was ++++, giving a dominant n=0 harmonic (about 85% of the power spectrum) when the mode is being tracked, with other harmonics appearing when the real-time tracking is lost between t=29.2sec and t=30.5sec.

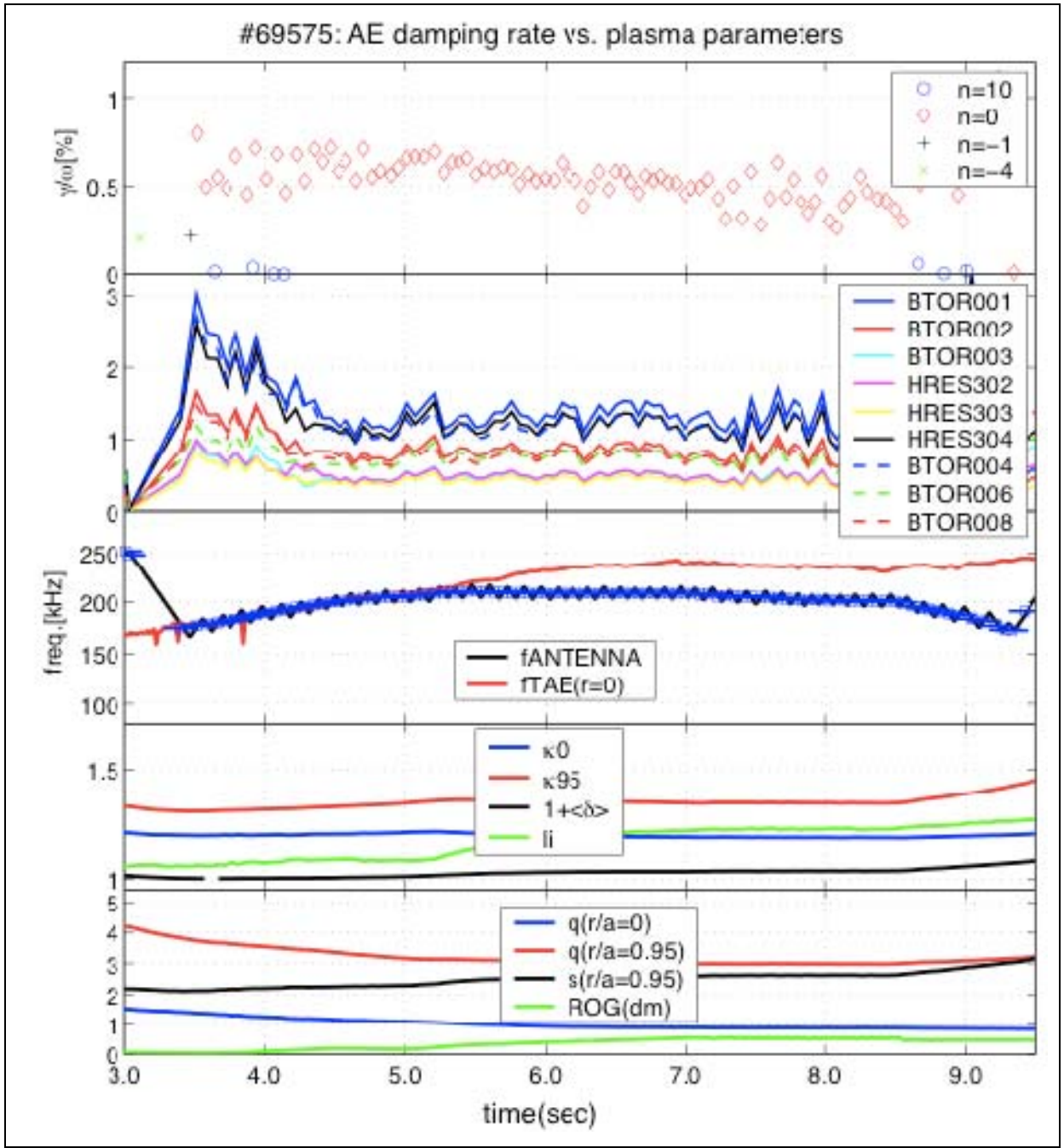

Figure 9. Mode frequency, damping rate and background plasma parameter for an ohmic limiter JET discharge where the four antennas were excited in the ++++ phasing configuration. The dominant harmonic in the driven and detected n-spectrum is the n=0 mode, with the n=10 mode most likely being an artefact of the SparSpec decomposition in toroidal harmonics. For the n=0 AE, the damping rate measured with the new antennas is essentially identical to that obtained with the old saddle coils in very similar experimental conditions. The labels BTOR and HRES indicate the synchronously detected signal measured at different magnetic pick-up coils (in arbitrary units).

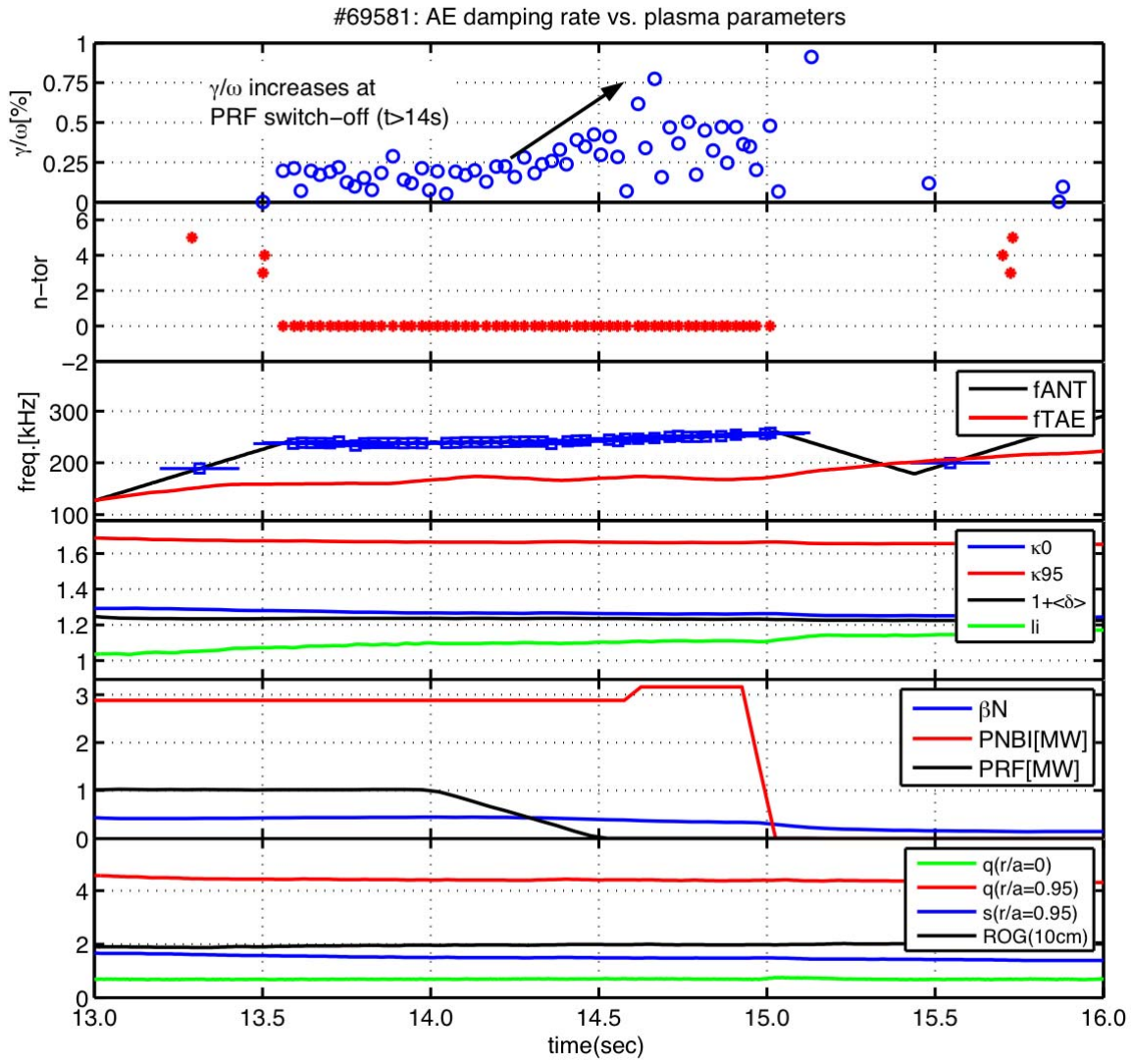

Figure 10. Mode frequency, damping rate and background plasma parameter during the additional heating phase (P_{NBI}~4MW, P_{RF}~1.5MW) of an X-point JET discharge with monotonic q-profile, with ROG~15cm and q_0~1. The antenna configuration spectrum was ++++, driving predominantly low-n modes. For the n=0 mode being tracked during the ICRF heating phase, we note that at the ICRF power switch-off (t>14sec) the damping rate increases, thus indicating a reduction in the fast ion drive. Other harmonics with higher n's are being detected outside the tracking phase.

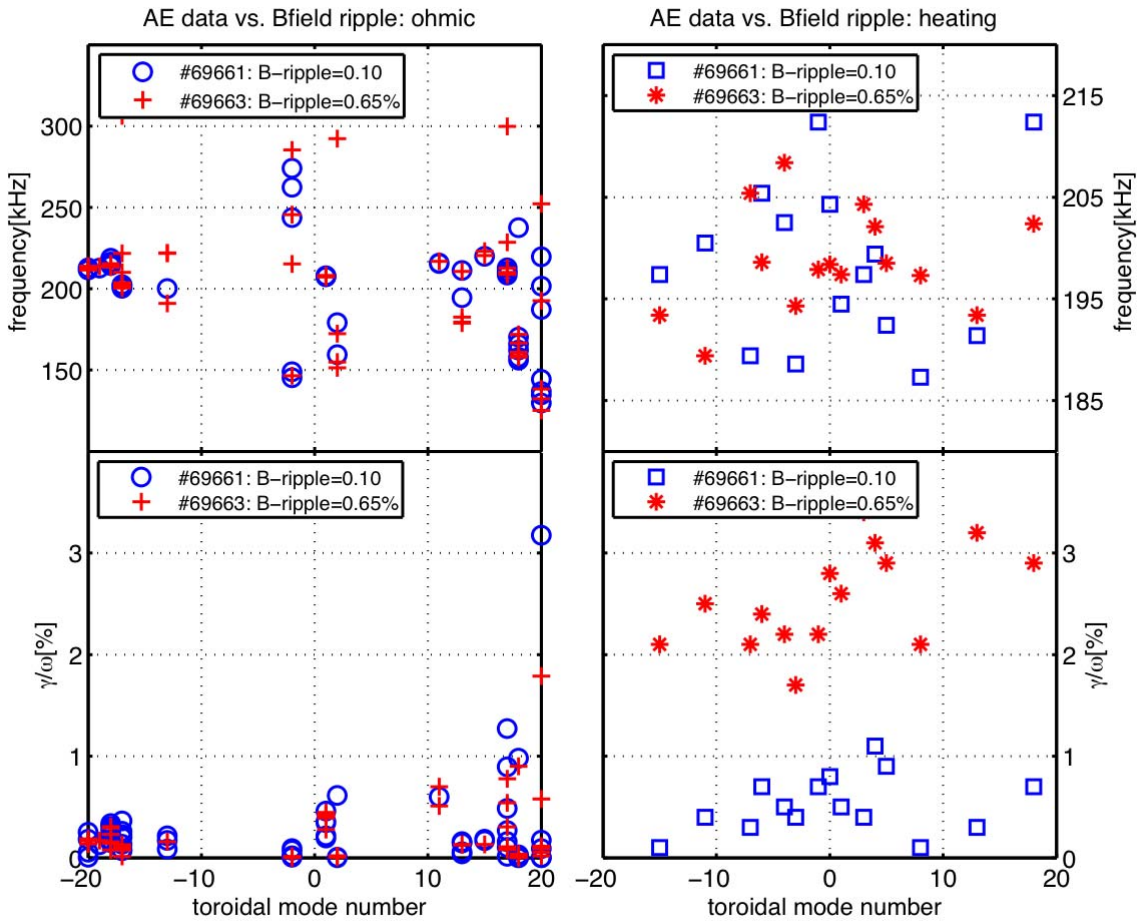

Figure 11. Mode frequency and damping rate for standard and high B-field ripple (0.1% and 0.65%, respectively), in two X-point JET discharges during the ohmic and high-power additional heating phase (P_{NBI}~10MW, P_{RF}~4MW and β_N~1). A larger γ/ω>2% is found during the NBI heating phase with the higher B-field ripple, whereas similar damping rates are obtained during the ohmic phase. Note that the measurements for modes with |n|>10 may be compromised by their amplitude being very close to the background noise level.

Figure 12a. One of the new active MAST AE antennas, installed in-vessel.

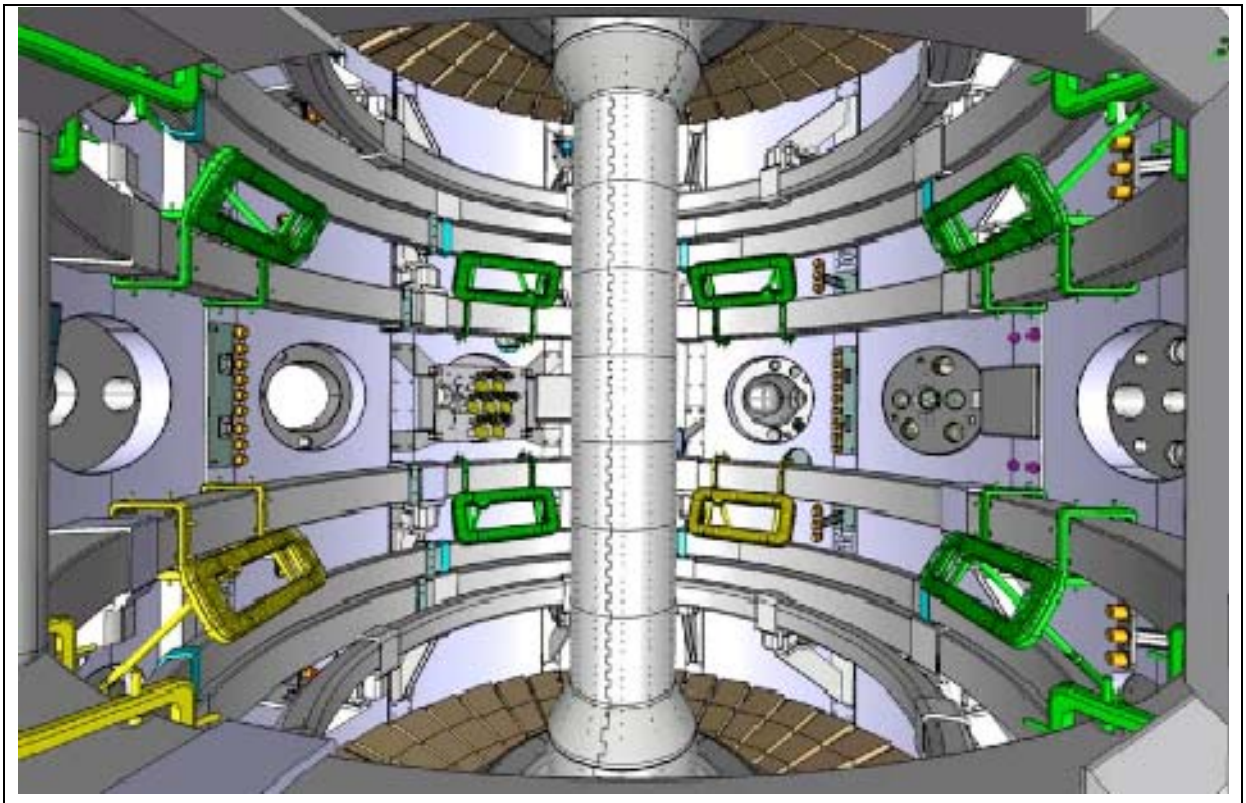

Figure 12b. Schematic view of the interior of MAST showing the in-vessel positions of the active AE antennas. The yellow antennas in the figure are those used in the initial trial installation, and correspond to those used in generating the results shown in Fig. 14.

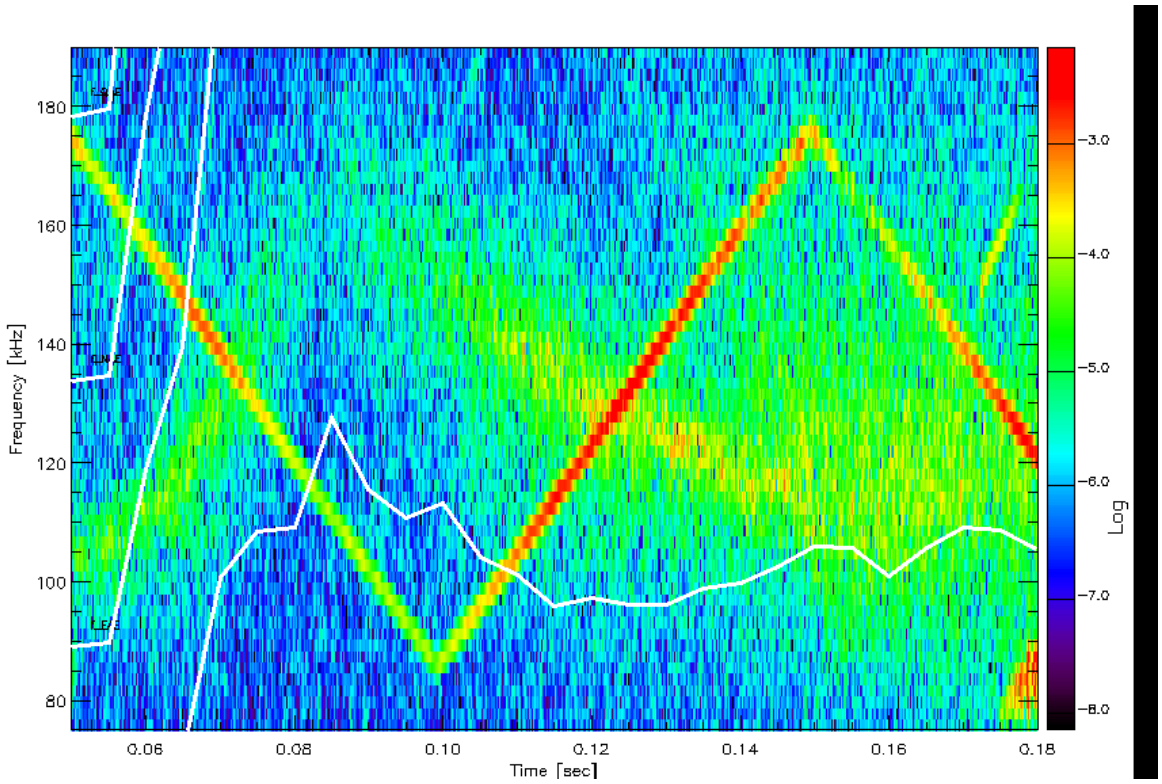

Figure 13. Magnetic spectrogram for MAST #18487 showing active AE diagnostic sweeping in frequency from 85kz to 180kHz and exciting a weakly damped mode at around 65ms and a strongly damped mode at around 120ms. The overlaid white lines approximately indicate the frequency range around which TAE modes and EAE modes may be expected to be excited.

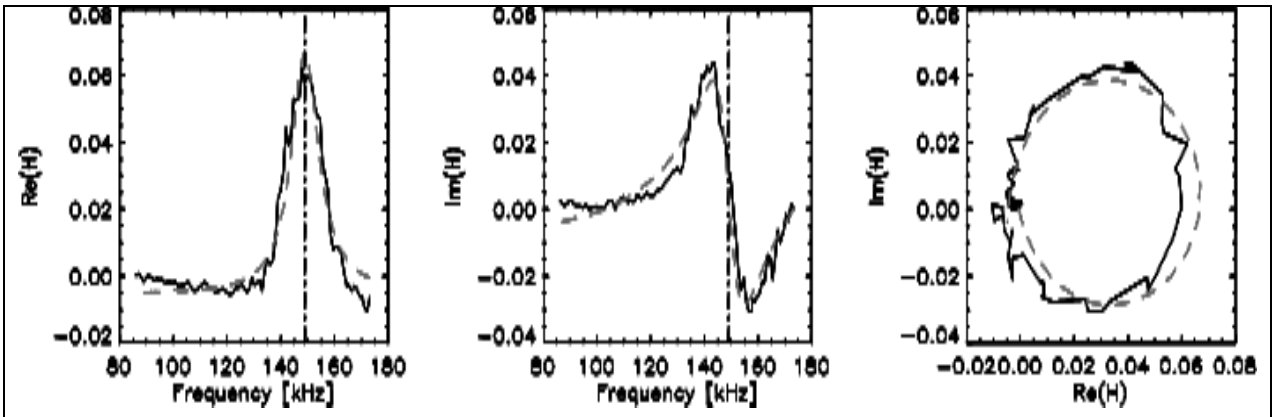

Figure 14. First data from MAST using the newly installed antennas: measured (solid lines) and fitted (dotted lines) transfer function for a magnetic pick-up coil for MAST #18487. A clear resonance is observed at 148.9kHz (indicated by the vertical dot-dash lines) with damping rate γ/ω=4.15%, but the toroidal mode number was not identified.